Desalination and Water Treatment
www.deswater.com
doi: 10.1080/19443994.2014.883045

52 (2014) 2811–2816
March

Taylor & Francis
Taylor & Francis Group

Research on optimal radius ratio of impellers in an oxidation ditch by using numerical simulation

Y.L. Liu*, W.L. Wei, B. Lv, X.F. Yang

State Key Laboratory of Eco-Hydraulic Engineering in Shaanxi, Xi'an University of Technology, XAUT, Xi'an 710048, Shanxi, China
Email: wei_wenli@126.com

Received 12 July 2012; Accepted 10 December 2013

ABSTRACT

Impellers are the main power source for oxidation ditches. Impeller radius has an important influence on the velocity distribution and the flow field structure in oxidation ditch channels. In this paper, the relation between the size of impeller radius and the structure of flow field in an oxidation ditch was studied by using the two-phase gas–liquid model and the 3D Realizable k–ε turbulence model. The pressure implicit with splitting of operators algorithm was used for the solution of velocity and pressure. The volume of fluid method was used to simulate the free surface. The research results show that when the ratio of the impeller radius to the diameter of the oxidation ditch channel bend, r/d, is 0.218, the percentage of the fluid with velocity greater than 0.3 m/s to the entire fluid is the greatest, and the length of the backflow region in straight channels is relatively shorter. The ratio of impeller radius to the diameter of an oxidation ditch channel bend, r/d, with a value of 0.218, is called the optimal impeller radius ratio.

Keywords: Oxidation ditch; Impeller; Optimal radius' ratio; Numerical simulation; Flow field

1. Introduction

Oxidation ditch is one of the main structures of sewage treatment plants. The flow structure of an oxidation ditch has important influences on the running efficiency of the oxidation ditch, which was studied by many domestic and foreign scholars using a lot of experiments and numerical simulations. Fan et al. [1] focused on the hydrodynamics of an oxidation ditch from the point of view of both experiments and simulations. The three-dimensional flow field in the oxidation ditch aerated with surface aerators like inverse umbrella was simulated with computational fluid dynamics (CFD). The two-fluid model and the standard k–ε model were used for the turbulent solid–liquid two-phase flow. Guo et al. [2] monitored the flow velocity and DO concentration in the outer channel of an orbal oxidation ditch system in a wastewater treatment plant in Beijing (China) under actual operation conditions, and analyzed the flow field and DO concentration distributions by fluid dynamic modeling. Simon [3] and Cao and Fu [4] studied some measures to improve flow field structures of oxidation ditches. Xu et al. [5] tested the

*Corresponding author.

Presented at the Second International Conference on Water Resources Management and Engineering (ICWRME 2012) Zhengzhou, China, 14–16 August 2012

hydraulic characteristics of the alternating aeration conditions of Carrousel oxidation ditch. Li et al. [6] studied on the flow characteristics under the action of aeration and impellers for oxidation ditches. In numerical simulation, Zhang et al. [7] and Jiang et al. [8] studied the flow field of oxidation ditch using CFD numerical model. Wang et al. [9] did some simulation and improvement on the bend flow field of oxidation ditches. Luo et al. [10] numerically simulated the oxidation ditch using three-dimensional model. Zhang et al. [11] did some structure optimizations of the oxidation ditch by numerical simulations using the three-dimensional flow model. Flow movement in an oxidation ditch is caused by the moving impellers, and the flow field structure is closely related to the factors of the impellers, such as radius, position, running speed, etc. The above researches do not relate to the optimization of impeller radius. This paper studies the relations between the size of the radius and the structure of flow fields in an oxidation ditch by using numerical simulation method to optimize impeller radius.

2. Definition of the optimal impeller

We study the relation between the size of impeller radius and the structure of flow field in an oxidation ditch under the same impeller position and running speed.

The oxidation ditch designing rule requires that the fluid average velocity is greater than 0.3 m/s. We take the percentage of the fluid with velocity greater than 0.3 m/s to the total fluid, P, as a variable, and the ratio of the impeller radius r to the bend radius d, r/d, as another dimensionless parameter. P increases with r/d under the same impeller position and running speed. When P gets to the greatest, the corresponding r/d is called the optimal impeller radius ratio.

3. Mathematical model

3.1. Governing equations

The unsteady 3D flow governing equations for continuity, momentum can be written as follows [12]:

$$\frac{\partial \rho}{\partial t} + \frac{\partial(\rho u_i)}{\partial x_i} = 0 \tag{1}$$

$$\frac{\partial(\rho u_i)}{\partial t} + \frac{\partial(\rho u_i u_j)}{\partial x_j} = -\frac{\partial p}{\partial x_i} + \frac{\partial}{\partial x_j}\left[\mu\left(\frac{\partial u_i}{\partial x_j} + \frac{\partial u_j}{\partial x_i}\right)\right] - \frac{\partial}{\partial x_j}(\rho\overline{u_i' u_j'}) + \rho g_i \tag{2}$$

$$-\rho\overline{u_i' u_j'} = \mu_t\left(\frac{\partial u_i}{\partial x_j} + \frac{\partial u_j}{\partial x_i}\right) - \frac{2}{3}\left(\rho k + \mu_t \frac{\partial u_i}{\partial x_i}\right)\delta_{ij} \tag{3}$$

where t is the time; x_i is the space coordinate in i ($i = x,y,z$)direction; p is the pressure; μ is the molecular kinematic viscosity; μ_t is the kinematic viscosity; g_i is the gravitational acceleration in i direction; u_i is the velocity component in i direction ($u_1 = u$, $u_2 = v$, $u_3 = w$); u_i' is the fluctuating velocity component in i direction ($u_1' = u'$, $u_2' = v'$, $u_3' = w'$); ρ is the density (in water ρ is equal to the water density; in the air ρ is equal to the air density); k is the turbulent kinetic energy.

For the estimation of the turbulence term $-\rho\overline{u_i' u_j'}$, a Realizable k–ε turbulence model is incorporated for the estimation of μ_t. The formulas for a 3D model are given as [12]:

Turbulent kinetic energy k equation:

$$\frac{\partial(\rho k)}{\partial t} + \frac{\partial(\rho k u_i)}{\partial x_i} = \frac{\partial}{\partial x_j}\left[\left(\mu + \frac{\mu_t}{\sigma_k}\right)\frac{\partial k}{\partial x_j}\right] + G_{kb} - \rho\varepsilon \tag{4}$$

Kinetic energy dissipation rate ε equation:

$$\frac{\partial(\rho \varepsilon)}{\partial t} + \frac{\partial(\rho \varepsilon u_i)}{\partial x_i} = \frac{\partial}{\partial x_j}\left[\left(\mu + \frac{\mu_t}{\sigma_\varepsilon}\right)\frac{\partial \varepsilon}{\partial x_j}\right] + \rho C_1 E\varepsilon - \rho C_2 \frac{\varepsilon^2}{k + \sqrt{v\varepsilon}} \tag{5}$$

where:

$$G_{kb} = \mu_t\left(\frac{\partial u_i}{\partial x_j} + \frac{\partial u_j}{\partial x_i}\right)\frac{\partial u_i}{\partial x_j},$$

$$\mu_t = \rho C_\mu \frac{k^2}{\varepsilon}, \quad C_1 = \max\left(0.43, \frac{\eta}{\eta + 5}\right),$$

$$\eta = (2E_{ij} \cdot E_{ij})^{1/2}\frac{k}{\varepsilon}, \quad E_{ij} = \frac{1}{2}\left(\frac{\partial u_i}{\partial x_j} + \frac{\partial u_j}{\partial x_i}\right)$$

$$C_u = \frac{1}{A_0 + A_s U^* k/\varepsilon}, \quad A_0 = 4.0, \quad A_s = \sqrt{6}\cos\phi,$$

$$\phi = \frac{1}{3}\cos^{-1}(\sqrt{6}W), \quad W = \frac{E_{ij}E_{jk}E_{ki}}{(E_{ij}E_{ij})^{1/2}},$$

$$E_{ij} = \frac{1}{2}\left(\frac{\partial u_i}{\partial x_j} + \frac{\partial u_j}{\partial x_i}\right), \quad U^* = \sqrt{E_{ij}E_{ij} + \tilde{\Omega}_{ij}\tilde{\Omega}_{ij}},$$

$$\tilde{\Omega}_{ij} = \Omega_{ij} - 2\varepsilon_{ikj}\omega_k, \quad \Omega_{ij} = \tilde{\Omega}_{ij} - \varepsilon_{ijk}\omega_k$$

where k and ε are turbulent kinetic energy and kinetic energy dissipation rate, respectively; σ_k, C_2, and σ_ε are empirical constants and have the value of 1.0 , 1.92, and 1.2, respectively.

The above equations with the corresponding boundary conditions according to actual problems constitute this problem to be solved.

3.2 Volume of fluid method

To describe the complicated surface between two fluids (air and water), the volume of fluid (VOF) method [4] is used. The VOF method introduces a VOF function F to define the water region. The meaning of the F function is the fractional volume of a cell occupied by water. In particular, a unit value of F corresponds to a cell full of water, while a zero value indicates that the cell contains no water. Cells with F value between zero and unity must then contain the free surface. The fractional function F can be evaluated as follows:

$$F = \frac{V_w}{V_c} \tag{6}$$

where V_w is the volume of water inside a cell and V_c is volume of the cell.

The time dependence of F is governed by the equation:

$$\frac{\partial F}{\partial t} + \frac{\partial (uF)}{\partial x} + \frac{\partial (vF)}{\partial y} + \frac{\partial (wF)}{\partial z} = 0 \tag{7}$$

There are a number of algorithms such as the donor–acceptor [5,6], etc. for the treating of the advection term in Eq. (7). In this study, we follow the method of Harvie and Fletcher [7].

According to the definition of the VOF function, the density and viscosity can be expressed in term of the fractional function F. The averaged values of density and viscosity can be determined respectively using the following equations:

$$\rho = (1 - F)\rho_\alpha + F\rho_w \tag{8}$$

$$U = (1 - F)u_\alpha + Fu_w \tag{9}$$

where ρ_α and u_α are the density and the viscosity of air, respectively; ρ_w and u_w are the density and the viscosity of water, respectively.

The system of Eqs. (1), (2), (7)–(9) can be applied directly to the region filled with air and water without any interpolation or extrapolation for the velocity or pressure at the interface. Accordingly, the effect of the variable of density is included.

4. Calculation region and grid

4.1. Calculated physical model

The side wall of the Carrousel oxidation ditch studied in this paper is 5 m high, 115 m long, the water depth is 4.5 m high. The capacity of the wastewater treatment is 25,000 m^3 each day. Three aeration impellers with a speed of 30 rpm are arranged at both ends of the oxidation ditch (see Fig. 1). In the numerical calculation, the computational domain is 109 m long, 34.6 m wide, and 6 m high. The single channel is 8.5 m wide; the radius of the small bend is 8.5 m, and of the big bend is 17 m. The thickness of the Carrousel diversion wall is 0.2 m. A, B, C, and D indicate the four straight channels. The region of calculation is shown in Fig. 1.

4.2. Grid generation

The computational grid in Fig. 2 is generated by the GAMBIT procedures; the pressure implicit with splitting of operators algorithm was used for the solution of velocity and pressure. The VOF method was used to simulate the free surface.

4.3. Initial conditions and mathematical model for the impellers

It was found that the inlet and outlet conditions have little influence on the flow field structure of the oxidation ditch, so they cannot be considered in the numerical calculation. The initial water depth is given as 4.5 m. The mathematical model of the impeller is adopted as the multiple reference frame model with sliding mesh method. Firstly, the multiple reference frame model is used to the initialization of the flow field, and then the sliding mesh is used for the computing to convergence.

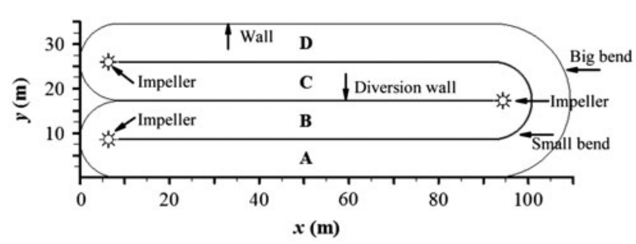

Fig. 1. Horizontal plan of the computational domain (unit: m).

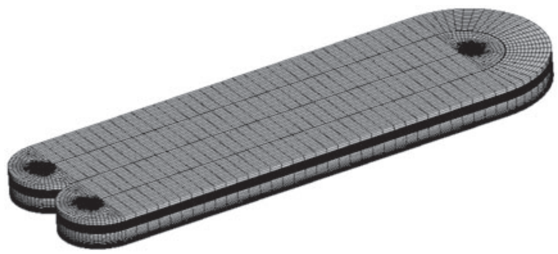

(a) Grid of the 3D computational domain

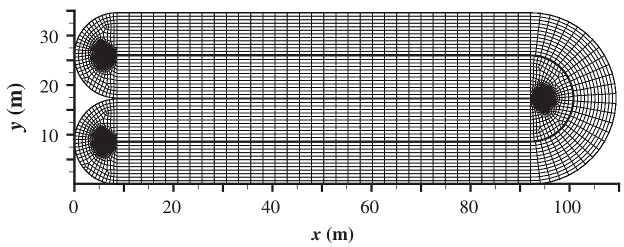

(b) Grid of the horizontal plan of the domain

Fig. 2. Grid of the computational domain.

5. Analysis of calculation results

5.1. Statistical analysis of the optimal radius ratio

The computed results for the five different radius (r/d = 0.145, 0.218, 0.291, 0.363, and 0.436) are taken as the statistical analysis. The designing rule requires that the average velocity in an oxidation ditch is greater than 0.3 m/s, according to which we obtain the optimal impeller radius.

The variable P indicates the percentage of the VOF with velocity greater than 0.3 m/s to the total fluid volume, and the dimensionless parameter $r/d$is the ratio of the radius r of an aeration impeller to the bend radius d. By using P and its correspondingr/d, the curve showing the increase of P with $r/d$is obtained in Fig. 3, from which we found that P increases with an increase of r/d at first and then decreases. When P gets to the biggest value, r/d equals to 0.218, which is called the optimal radius ratio of the aeration impellers.

From Fig. 3 we find that the influencing range of the water flow is small when the impeller radius is small under the same impeller position and running speed. The influencing range increases with an increase of the impeller radius, but when the impeller radius increases to a certain extent, the too large impeller will affect the flow capacity through the bend, and the percentage of fluid with velocity greater than 0.3 m/s to the entire fluid is stable at around 90%.

An oxidation ditch consists of bends and straight channels. The thickness of the wall of straight chan-

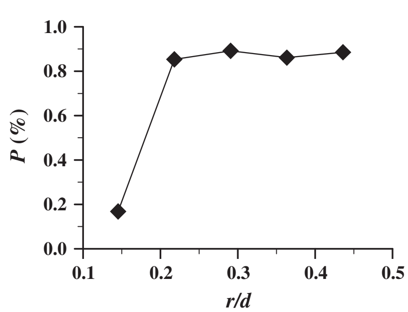

Fig. 3. P varying with r/d.

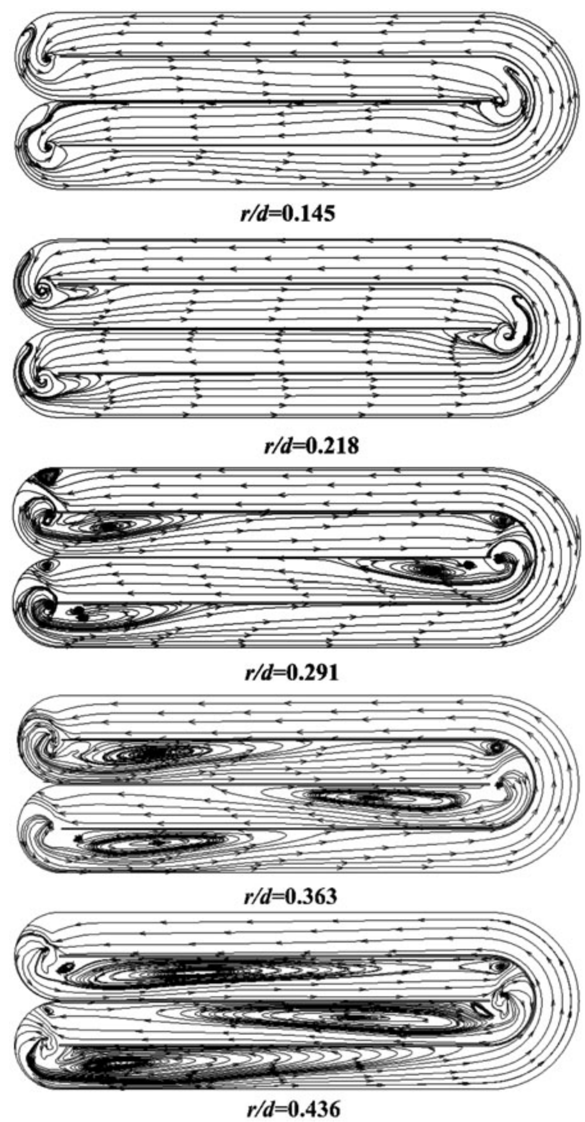

Fig. 4. Computed streamlines at 2.5 m water depth.

nels is much smaller than the radius of the bends. When water runs from bends into straight channels, recirculation forms near the straight wall ends, and the recirculation region is unfavorable for running operation of an oxidation ditch. Under the different values of r/d, the computed streamlines at the same water depth 2.5 m were plotted in Fig. 4.

Fig. 4 shows that there is almost no recirculation region near the wall ends when the radius ratio is very small, but with the increase of radius ratio, the recirculation region near the wall ends appears, and its length is much increased; and when the radius ratio is of 0.436, the length of the recirculation zone is almost equal to the length of straight channel.

The fluid speed at the impeller blade tip will increase with the increase of the impeller radius at the same rotation speed, which results in the velocity distribution at outlets of the bends being extremely non-uniform: the velocity near the wall is very small, and far away from the wall is large; at the same time near the bend exit section, the action of inertia force of flow can lead to the velocity distribution near the bend exit sections being non-uniform, so the recirculation zone forms, and the length of the recirculation zone has relations with the non-uniform velocity distribution near the bend exit sections; the more non-uniform the velocity distribution is, the more long the recirculation zone becomes. Similarly, with the increase of the impeller radius, the water entrainment near the impeller will be strengthened, which will have much influence on the flow structure of oxidation ditches.

5.2. Analysis of the flow structure with the optimal radius ratio

The flow structure of an oxidation ditch has great influence on its running efficiency. The velocity vectors at the horizontal plan with a depth of 2.5 m are plotted in Fig. 5.

The streamline chart with $r/d = 0.218$ in Fig. 4 and the velocity vectors in Fig. 5 show that on the horizontal plan of a depth of 2.5 m, near the outlet cross-sections of the bends exist smaller recirculation, but the rest flow runs smoothly.

To study the flow movement on the cross-sections of the channels, the streamlines on cross-sections of $x = 10$ m and $x = 50$ m are plotted in Fig. 6.

Fig. 6 shows that obvious transverse circulation exists in the lateral profiles due to the shape of the oxidation ditch, especially near the water outlet sections of the bends.

The ratio of the velocity in the vertical direction to that in the horizontal direction v_y/v_x is taken as a measure of the strength of the lateral movement in an oxidation ditch, the change of which along the depth direction under the optimal impeller radius, at $x = 21.35$ m, $x = 46.35$ m, and $x = 71.35$ m in Channel A,

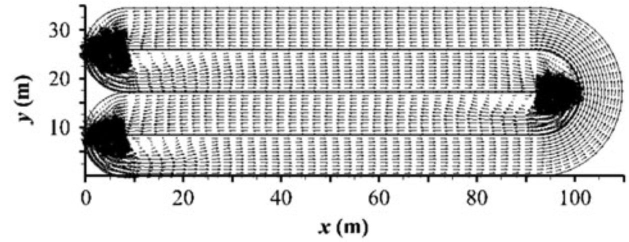

Fig. 5. Computed vectors with a depth of 2.5 m.

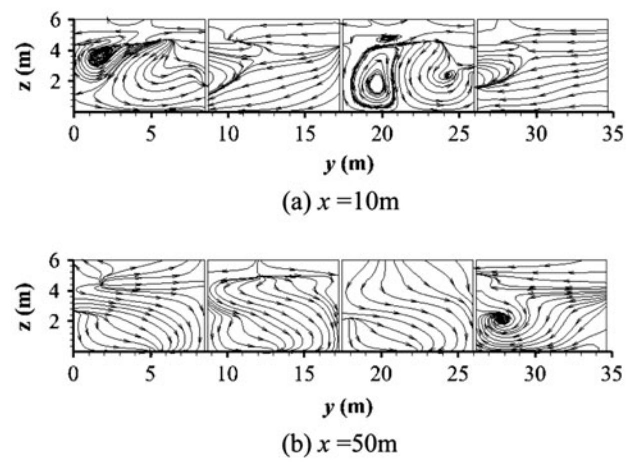

Fig. 6. Streamlines on cross-sections of $x = 10$ m and $x = 50$ m. (a) $x = 10$ m, (b) $x = 50$ m.

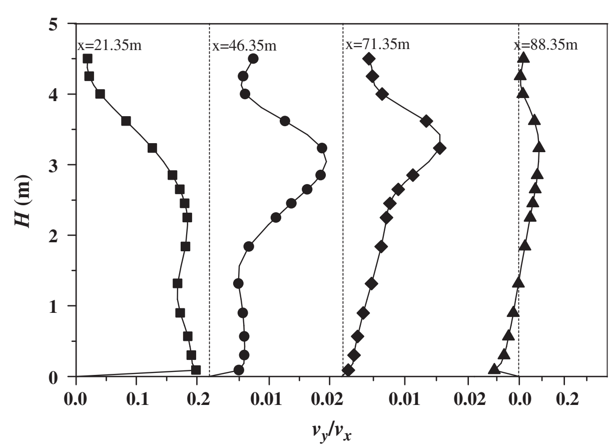

Fig. 7. Comparisons of transverse flow motion intensity along the depth-direction.

and $x = 88.35$ m in Channel D, are plotted in Fig. 7. The curves share the same vertical coordinate H of water depth, and the horizontal coordinates are independent, and separated with dotted lines at 0-points.

Fig. 7 shows that there is transverse motion of flow in an oxidation ditch, near the smaller bend exit end with $x = 21.35$ m, due to the influence of the impeller, the lateral water speed can reach to the maximum velocity of about 20% the longitudinal velocity, and near the outlet of the bigger bend end with $x = 88.35$ m, the flow transverse velocity can also reach about 10% the longitudinal velocity. Relatively speaking, in the straight channels of the oxidation ditch, away from the small bend outlet end, the lateral movement of flow is much weaker; but in the region with a depth of 3–4 m, the transversal movements is much stronger, the largest value is less than 2% the longitudinal speed.

6. Conclusions

The size of impeller radius has important influences on the structure of flow field in an oxidation ditch. Under the same impeller position and running speed, the optimal impeller radius ratio r/d is 0.218, with which the percentage of fluid with velocity greater than 0.3 m/s to the entire fluid is the greatest, and the length of the backflow region in straight channels is shorter. Impellers with optimal impeller radius ratio make the flow structure of an oxidation ditch be favorable for the running efficiency of oxidation ditches.

Acknowledgments

This work was supported by the National Natural Science Foundation of China (Grant No. 51178391), Special funds for the development of characteristic key disciplines in the local university by supported the central financial (Grant No. 106-00X101, 106-5X1205) and the Shanxi Province key subject construction funds.

References

[1] L. Fan, N. Xu, Z. Wang, H. Shi, PDA experiments and CFD simulation of a lab-scale oxidation ditch with surface aerators, Chem. Eng. Res. Des. 88 (2010) 23–33.

[2] X. Guo, X. Zhou, Q. Chen, J. Liu, Flow field and dissolved oxygen distributions in the outer channel of the orbal oxidation ditch by monitor and CFD simulation, J. Environ. Sci. 25(4) (2013) 645–651.

[3] S. Simon, Prediction of mean circulation velocity in oxidation ditch, Environ. Technol. 22(2) (2001) 195–204.

[4] R.-Y. Cao, J.-Z. Fu, Measures for improving distribution in oxidation ditch, Chin. Water Wastewater 17(2) (2001) 16–18.

[5] D.-y. Xu, D.-j. Zhang, Z.-s. Pang, L.-s. Guo, Determination of hydraulic characteristics of carrousel oxidation ditch under alternating aeration conditions, China Water Wastewater 24(4) (2008) 95–99.

[6] Z.-j. Li, J.-j. He, Y. Xu, H.-h. Song, Characteristics of flow fields in oxidation ditches under action of aeration turntables, J. Hohai Univ. (Natural Sciences) 39(2) (2011) 143–147.

[7] Y. Zhang, W.-d. Huang, Q.-z. Gou, Application of computational fluid dynamics in design of oxidation ditch, Ind. Water Wastewater 40(1) (2009) 49–53.

[8] C.-y. Jiang, W.-d. Huang, G. Wang, Numerical Computation of flow fields in an oxidation ditch by computational fluid dynamics model, Environ. Sci. Technol. 33(8) (2010) 135–140.

[9] H.-j. Wang, Y.-b. Guo, Y.-x. Hu, Numerical simulation of flow fields of oxidation ditch bends, Energy Environ. 6 (2009) 10–12.

[10] L. Luo, W. Li, Y. Deng, Numerical simulation of a combined oxidation ditch flow using 3D k-ε turbulence model, J. Environ. Sci. 17(5) (2005) 808–812.

[11] Z. Zang, H. Chai, B. Li, Simulation on three-dimensional flow field and improvement on structure of anoxic zone of A~2O oxidation ditch, Chin. J. Environ. Eng. 1 (2012) 46–50.

[12] W. Wei, H. Dai, Turbulence Model Theory and Engineering Applications, Shanxi Science and Technology Press, Xian, 2006.